Binary Mixtures of Diblock Copolymers: Phase Diagrams with a New Twist

An-Chang Shi and Jaan Noolandi*

Xerox Research Centre of Canada, 2660 Speakman Drive, Mississauga, Ontario, Canada L5K 2L1

Received December 6, 1994; Revised Manuscript Received February 15, 1995®

ABSTRACT: The phase behavior of mixtures of two monodisperse diblock copolymers made up of A and B monomer units is investigated using self-consistent mean-field theory. A new scheme for phase structure analysis, namely, a "phase cube", is introduced and used to study the global symmetries with respect to the chemical compositions and the volumes fractions of the two components. Within the global scheme local density profiles for selected structures and molecular parameters are calculated and used to study the self-organization of the polymer chains. Several particularly interesting structures, such as the bilayer and inverted spherical phases, are investigated. Some possible uses for the inverted spherical phase in local thermodynamic equilibrium with polymeric components different from the A and B blocks of the copolymers are suggested.

1. Introduction

One of the ultimate goals in studies of block copolymers is the development of methods to determine polymer morphology for materials applications. The phase behavior of diblock copolymers can be controlled by synthesizing precisely tailored diblock copolymers. Another route to control block copolymer morphologies is through polymer blending, in which two or more copolymers with different morphologies are mixed together to get a desired morphology. Furthermore, mixtures of diblock copolymers are interesting because of their potential to form new types of ordered phases and as a testing ground for theoretical models which have been developed for one-component systems. New equilibrium morphologies in weakly segregated diblock copolymers continue to be found,[1] and, in general, blends of diblock copolymers with each other as well as with homopolymers will attract the attention of polymer scientists for some time to come.[2−7]

What has been lacking on the theoretical side is a systematic attempt at understanding the phase behavior of even a simple system such as a binary mixture of two types of monodisperse diblock copolymers composed of A and B monomer units. Due to the large number of controlling parameters (two molecular weights, two chemical compositions, temperature, and polymer volume fractions), a very rich phase behavior is expected for these binary mixtures. The phases of diblock copolymer melts are very well described by mean-field theory. Many methods have been developed to solve the mean-field equations for single-component diblock copolymer melts.[8−10] The methods are usually applicable either for the strong segregation limit[9] or for the weak segregation limit,[8] both involving specific assumptions about the polymer density profiles. An exact approach, which neither involves *a priori* assumptions about the shape of the equilibrium density profiles nor truncates the free energy, corresponds to solving the mean-field equations numerically.[10] For the binary mixtures of diblock copolymers, an analytic theory in the strong segregation limit has been developed and applied to the lamellar and cylindrical phases of the mixtures.[11] Mixing of diblock copolymers has been shown to have large effects on the self-assembly of diblock copolymer monolayers and bilayers in the strong segregation limit.[12] We have launched a systematic study of the phase behavior for diblock copolymer mixtures using the self-consistent mean-field theory. In an earlier paper,[13] we studied binary mixtures of long diblock copolymers and a small amount of short diblock copolymers and demonstrated that the phase behavior of the system can be altered by the addition of the short diblocks. In this paper, we propose a phase diagram scheme (a phase "cube") to explore the phase behavior of binary diblock copolymer mixtures systematically. The theoretical calculations are based on a self-consistent mean-field computational technique described earlier.[13] We consider only the standard lamellar, cylindrical, and spherical structures for simplicity, but even within this limited range of symmetries, we find interesting results such as the inverted spherical phase and the bilayer structure to be described later. We will restrict ourselves to the cases where the two diblock copolymers are of the same lengths, thus concentrating on the effects of chemical composition and volume fractions on the phase behavior. Extension of our calculation to general cases is straightforward. We discuss both the weakly segregated and strongly segregated cases. The self-organization of the diblock copolymer chains in the different structures is explored by density profile−structure diagrams. The various regions of stability of the different structures are explored as a function of copolymer composition ratios and volume fractions.

Besides the attempt at a systematic understanding of binary blends of diblock copolymers, we explore possible applications of some of these phases. This is partly motivated by recent interesting work of Cohen and co-workers[14−16] on microphase-separated domains of organometallic block copolymers. Here the morphology and size of metal- and semiconductor-containing microdomains have been studied for different copolymer compositions and block molecular weights. For the inverse spherical structure we discuss later, the possibility of using homopolymers as carriers and/or swelling agents for additives in spherical microdomains may extend the range of processing methods for preparing these materials. For example, the option exists of using homopolymers which are more incompatible with the matrix block than the microdomain block to prepare

® Abstract published in *Advance ACS Abstracts,* April 1, 1995.

0024-9297/95/2228-3103$09.00/0 © 1995 American Chemical Society

thin films of diblock copolymer AB/homopolymer A/homopolymer C which are in local, but not global, equilibrium. An application of these kinds of structures may be to 3D computer memory devices,[17] which involve the concentration of dyes into microdomains.

The organization of the paper is as follows: In section 2 the model system and the method used in the study are introduced, a discussion on the general phase diagram for binary mixtures of diblock copolymers is given, and a comparison between the weakly and strongly segregated regimes is made. Polymer density–profile–structure diagrams are shown in section 3, and section 4 focuses on the inverse spherical structure in local and global thermodynamic equilibrium. The conclusions are given in section 5. The details of the mean-field theory and associated computational techniques are reviewed in the appendix of ref 13 and will not be repeated here.

2. Phase Diagram for Binary Mixtures

We consider two types of AB diblocks, with chemical compositions $f_1 = Z_{1A}/Z_1$ and $f_2 = Z_{2A}/Z_2$ and a Flory–Huggins interaction parameter χ between the A and B units. Here Z_1 and Z_2 are the degrees of polymerization of the two diblock copolymer chains and Z_{1A} and Z_{2A} are the degrees of polymerization of the A blocks for the first and second components. The binary mixture itself is composed to two monodisperse components, with $1 - \phi$ as the volume fraction of the first component and ϕ as the volume fraction of the second component. In order to concentrate on the effects of the chemical compositions (f_1 and f_2) and the polymer volume fractions (ϕ), the degrees of polymerization of the two components are assumed to be equal, $Z_1 = Z_2 \equiv Z$. This leads to an anomalously high degree of symmetry in the phase diagram; however, if $Z_1 \approx Z_2$, we expect that the topology of the phase diagrams remains the same, even though the precise symmetries for $Z_1 = Z_2$ will be broken.

The model system is studied by using the self-consistent mean-field theory described earlier.[13] For a given set of parameters $\{\chi, Z, f_1, f_2, \phi\}$, the self-consistent-field theory is solved for the lamellar, cylindrical, and spherical structures. The equilibrium structure is determined by minimizing the free energy density with respect to the domain sizes of the structure. This procedure is repeated for all values of f_1, f_2, and ϕ. The phase diagram is then constructed by analyzing the free energies of the different structures.

The main issue is the best way to present the result for a system with a large number of variables. We have chosen the main variables to be the chemical compositions of the two components (f_1 and f_2) and their volume fractions (ϕ). Most of the calculations we have carried out are for $\chi Z = 20$, with $\chi = 0.05$ and $Z = 400$, in the crossover region between the weakly and strongly segregated regimes for diblock copolymer melts. We also present some results in the strongly segregated regime, for $\chi Z = 80$, with $\chi = 0.2$ and $Z = 400$, where the phase diagram becomes independent of χZ.

The phase diagram can be presented in the form of a cube, shown in Figure 1. The bottom plane corresponds to a one-component system with phase boundaries which are vertical, since the volume fraction of the second component, ϕ, is zero. The top plane corresponds to another one-component system with phase boundaries which are horizontal, since the volume fraction of the first component, $1 - \phi$, is zero. Between the bottom plane and the top plane the phase diagram twists in a way which is characteristic of a binary diblock copolymer blend, with the middle plane being the one of greatest symmetry. Due to the equivalence of A and B blocks, the center of each plane is a point of inversion symmetry in the plane ($f_1 \leftrightarrow 1 - f_1$, $f_2 \leftrightarrow 1 - f_2$), and this symmetry will be broken if the two blocks are of different sizes. Due to the equivalence of the two components ($Z_1 = Z_2$), the center of the cube is also a point of inversion symmetry in the cube ($f_1 \leftrightarrow f_2$, $\phi \leftrightarrow 1 - \phi$), and this symmetry will be broken for $Z_1 \neq Z_2$. The white dots indicate the intersections of the vertical plane defined by $f_1 = f_2$, which passes through two edges of the cube ($f_1 = 0$, $f_2 = 0$ and $f_1 = 1$, $f_2 = 1$), and the phase boundaries in the individual horizontal planes. Since $f_1 = f_2$ in this vertical plane and $Z_1 = Z_2$, the blend reduces to a one-component system, with ϕ being a redundant variable. Hence, the positions of the white dots are the same in all the horizontal planes. Therefore, these points are structural fixed points in the phase diagram. As mentioned earlier, if $Z_1 \approx Z_2$, the point symmetries are approximate, but the topology of the phase boundaries is the same as for the highly symmetric case with $Z_1 = Z_2$.

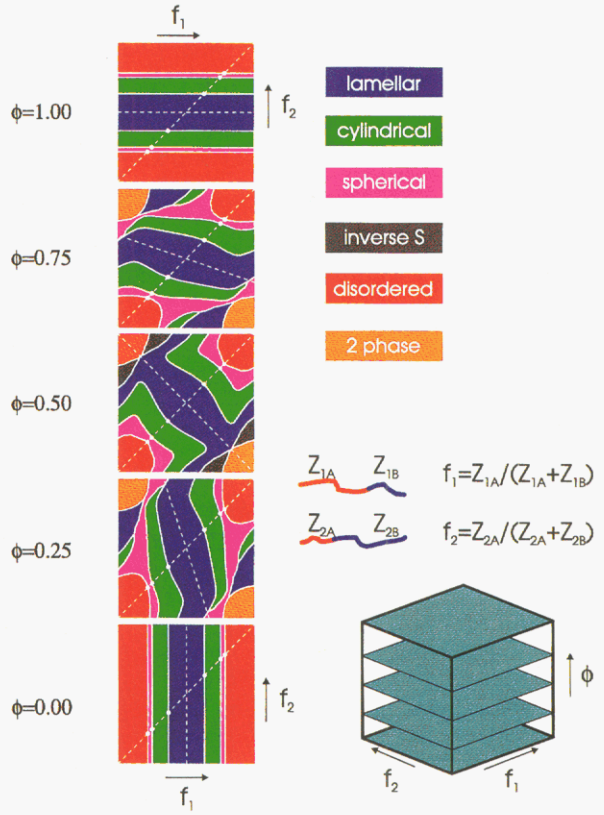

Figure 1. Calculated phase diagram "cube" for binary mixtures of diblock copolymers for the weakly segregated case, with $\chi = 0.05$ and $Z_1 = Z_2 = 400$.

Figure 2 shows the detail of the cut through the cube at $\phi = 0.25$. The dashed line sloping to the left is defined by $f = f_1(1 - \phi) + f_2\phi = 0.5$, where f is the total volume fraction of A blocks in the mixture. Simple volume-filling considerations lead to the conclusion that the system should assume a lamellar structure in the vicinity of this line. Figure 2 shows that this is indeed the case, except for the regions close to $f_2 = 0$ or $f_2 = 1$, *i.e.*, mixtures of one diblock copolymer with another extremely asymmetric diblock copolymer. Another dashed line (defined by $f_1 = f_2$) connecting the two corners corresponds to a one-component system. The

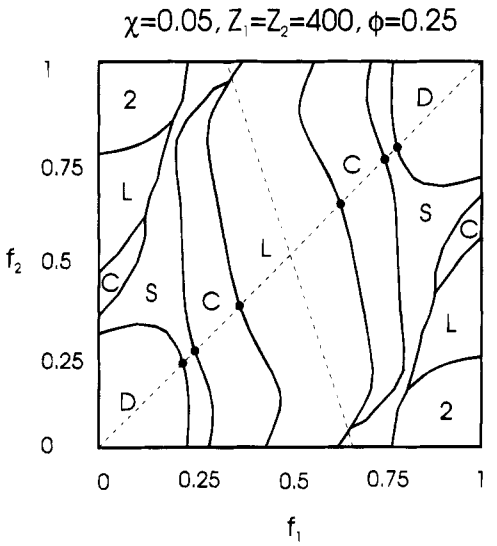

Figure 2. Detail of the calculated phase diagram shown in Figure 1, for the horizontal plane corresponding to $\phi = 0.25$.

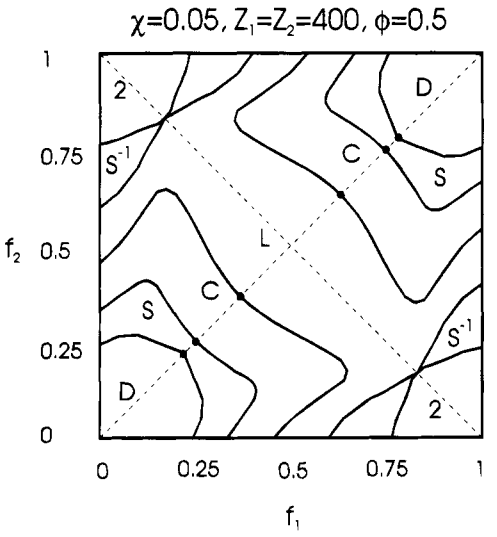

Figure 3. Detail of the calculated phase diagram shown in Figure 1, for the horizontal plane corresponding to $\phi = 0.5$.

sides of the square indicate mixtures where one of the two components is a homopolymer. Figure 3 details the cut through the cube at $\phi = 0.5$ and shows a highly symmetric structure for the phases of different symmetries. Of particular interest is the inverted spherical phase, labeled S^{-1}, which does not appear in Figure 2 for $\phi = 0.25$. Figure 4 shows the cut through the cube at $\phi = 0.75$. This diagram can also be obtained through point inversion of the diagram for $\phi = 0.25$ through the center of the cube. Detailed structural information about these phases is contained in the polymer density profiles, which will be discussed later.

Figure 5 shows the phase diagram for a strongly segregated system, with $\chi = 0.2$, $Z = 400$, and $\phi = 0.25$. Comparison with Figure 2 shows that the strongly segregated blend has much smaller two-phase and homogeneous regions and that the phase boundaries are more vertical. Figure 6 for the strongly segregated system with $\chi = 0.2$ also contains the inverted spherical phase in a narrow region bounded by the edges of the phase diagrams for the homopolymer/block copolymer mixtures.

The calculated phase diagram can be understood in terms of the interfacial spontaneous curvature and the

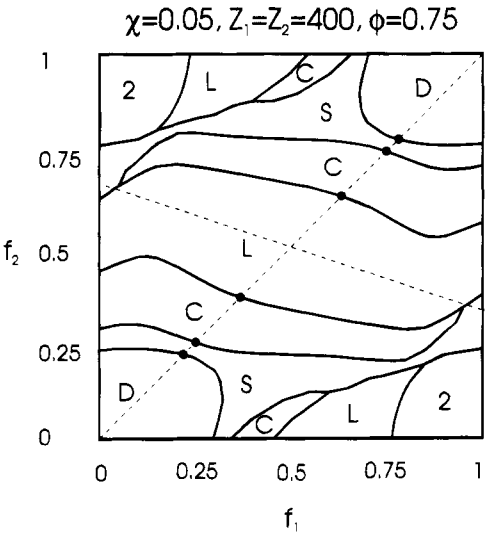

Figure 4. Detail of the calculated phase diagram shown in Figure 1, for the horizontal plane corresponding to $\phi = 0.75$.

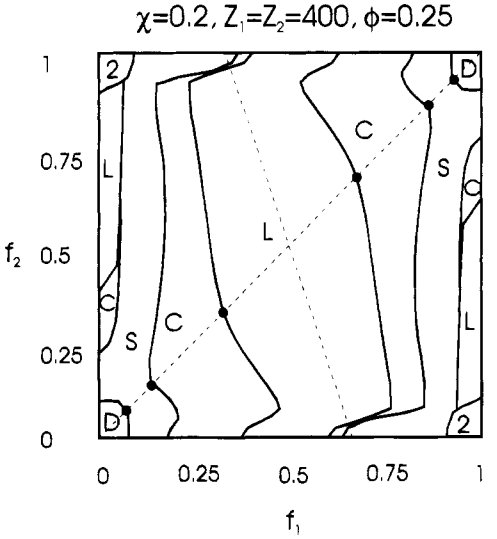

Figure 5. Detail of the calculated phase diagram for the strongly segregated case of binary mixtures of diblock copolymers, with $\chi = 0.2$, $Z_1 = Z_2 = 400$, and the horizontal plane corresponding to $\phi = 0.25$.

segregation of the diblocks. The spontaneous curvature of the interfaces is determined by the chemical compositions of the diblocks at the interfaces. If the diblocks are completely segregated, the spontaneous curvature is proportional to the total chemical composition $f = (1 - \phi)f_1 + \phi f_2$ and the phase boundaries will be determined by f only; *i.e.*, the phase boundaries will be parallel to each other. The segregation of the diblocks is determined by the chemical compositions f_1 and f_2. When f_1 and f_2 are close to 0.5, the diblocks are segregated to the interfaces. This explains the approximately parallel phase boundaries in the interior of the f_1–f_2 phase diagrams. On the other hand, when either f_1 or f_2 is close to 0 or 1, the highly asymmetric diblocks are localized in the middle of the domains, as will be demonstrated in the next section, and the interfacial spontaneous curvature is no longer determined by the total chemical composition f. For example, when $f_1 = 1$, the spontaneous curvature of the interfaces is determined by f_2. The appearance of the spherical, bilayer lamellar, and inverse spherical phases can be attributed to the change of the interfacial curvature with f_2.

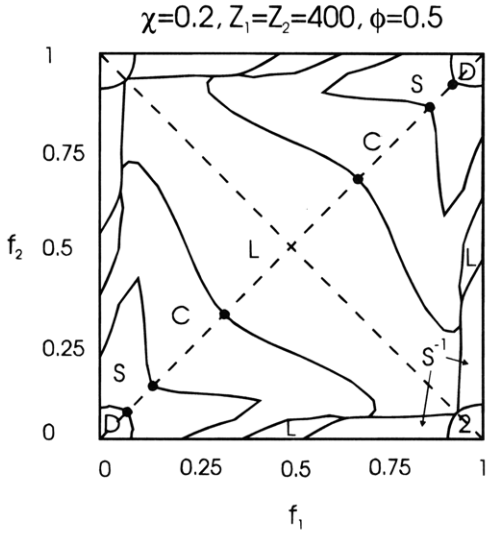

Figure 6. Detail of the calculated phase diagram for the strongly segregated case of binary mixtures of diblock copolymers, with $\chi = 0.2$, $Z_1 = Z_2 = 400$, and the horizontal plane corresponding to $\phi = 0.5$.

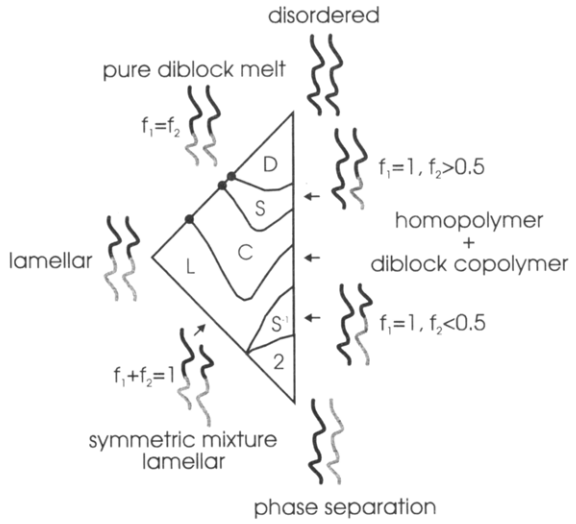

Figure 7. One-quarter of the phase diagram shown in Figure 3 for the weakly segregated case of binary mixtures of diblock copolymers. The arrows indicate the positions on the perimeter of the diagram where density profile calculations were carried out.

3. Polymer Density Profile–Structure Diagrams

In order to understand the self-organization of the polymer chains in the binary mixtures, it is helpful to calculate the density profiles and to relate the density profiles to the equilibrium structures. To study the density profiles associated with the various structures, we will focus on one-quarter of the symmetric phase diagram shown in Figure 3 for $\chi = 0.05$, $Z_1 = Z_2 = 400$, and $\phi = 0.5$. This section of the complete phase diagram is bounded by the straight lines ($f_1 = f_2$; $f_1 + f_2 = 1$; and $f_1 = 1$) and is shown in Figure 7. The structures inside the triangle in the different phases are similar to the corresponding phases around the perimeter. Practically, polymer morphology control can be achieved by blending the diblock copolymers whose properties are determined from the phase diagram. In what follows we will discuss the polymer density profiles and the diblock structures for the phases around the perimeter of Figure 7.

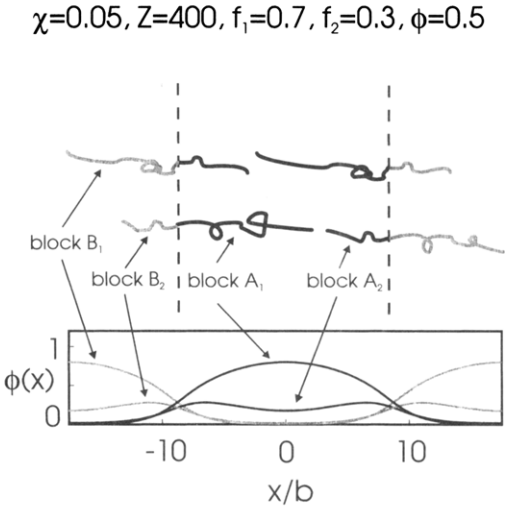

Figure 8. Structure–density profile diagram for a symmetric mixture of diblocks with $f_1 + f_2 = 1$, corresponding to a lamellar phase. All the distances in our calculations are measured in terms of the Kuhn length b.

The simplest case is the line $f_1 = f_2$. For the mixtures of equal length diblocks, this line corresponds to a pure diblock melt. The phases are therefore controlled by the chemical composition $f_1 = f_2$, and the phase transition sequence is the well-known one: lamellar to cylindrical to spherical to homogeneous when $f_1 = f_2$ changes from 0.5 to 1.

For the case $f_1 + f_2 = 1$, the system is a symmetric binary mixture. Due to the symmetry of the system, the diblocks form a lamellar structure, shown in Figure 8. The lamellar structure arises from the complementary short and long blocks of the copolymer fitting together, on the average, to give a domain of uniform width. As seen in the figure, the density profile of the short blocks has a dip in the middle of the domain, where the long block density profile has a maximum. The two extreme values of f_1 along this line are $f_1 = 0.5$ and $f_1 = 1$, corresponding to a pure symmetric diblock melt and a pure homopolymer A/homopolymer B mixture. Therefore, increasing f_1 along the straight line $f_1 + f_2 = 1$, displayed in the phase diagram Figure 7, the lamellar structure eventually becomes unstable and the system separates into two phases. Figure 9 shows the evolution of the free energy for this type of instability, which results in phase separation at $f_1 \simeq 0.83$ for the given chain parameters. In Figure 10 we see that the range of stability of the lamellar phase is greater for larger χ, a result due to the larger interfacial tension in this case, which provides a greater thermodynamic driving force for stretching the highly asymmetric diblocks into a lamellar structure.

For the case $f_1 = 1$, the system is an AB diblock and A homopolymer mixture. The two extreme values of f_2 are $f_2 = 1$, corresponding to a homogeneous homopolymer A melt, and $f_2 = 0$, corresponding to a phase-separated homopolymer AB mixture. Decreasing f_2 from 1 to 0 will, therefore, drive the system from the pure A melt to a phase-separated AB mixture, with the spherical, cylindrical, lamellar, and inverse spherical structures as intermediate phases. Figure 11 shows the density profiles for the top arrow along the vertical line of the phase diagram shown in Figure 7. Here $f_1 = 1$ and $0.76 > f_2 > 0.66$, corresponding to a mixture of homopolymers and diblock copolymers, which forms a spherical structure. The B blocks form well-defined spherical domains, and the A homopolymer disperses

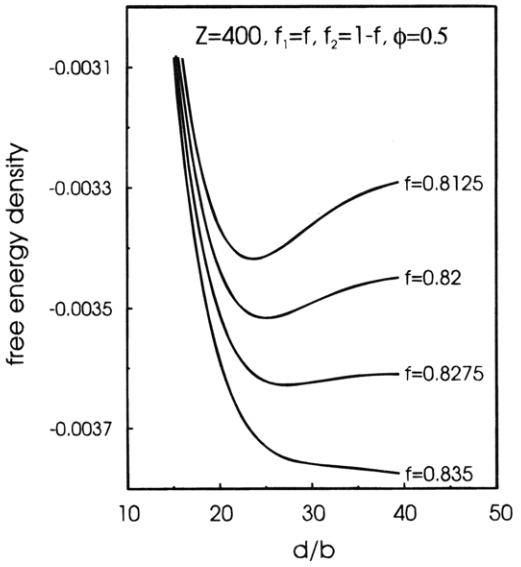

Figure 9. Free energy of the symmetric lamellar phase as a function of the lattice parameter d, when moving toward the two-phase region along the line $f_1 + f_2 = 1$ shown in Figure 7.

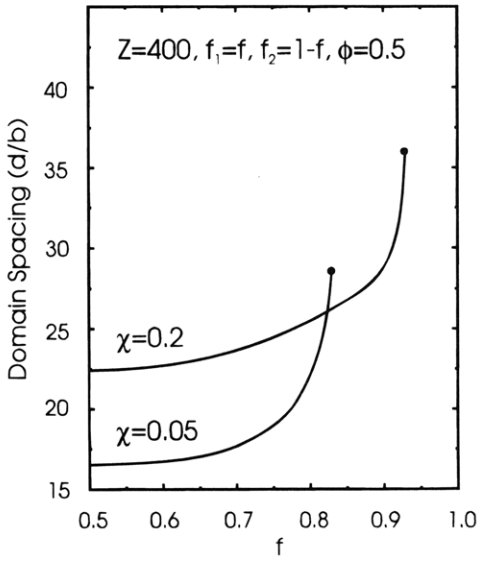

Figure 10. Domain spacing for the symmetric lamellar phase as a function of the asymmetry parameter, f, for both the weakly ($\chi = 0.05$, $Z = 400$) and strongly ($\chi = 0.2$, $Z = 400$) segregated cases when moving toward the two-phase region along the line $f_1 + f_2 = 1$ shown in Figure 7.

into the matrix formed by the A blocks of the copolymer. Decreasing f_2 from the value corresponding to this spherical phase drives the system into a cylindrical phase ($0.66 > f_2 > 0.54$), with similar molecular organization as the spherical phase, except that the spheres are replaced by cylinders. Decreasing f_2 further, the system assumes a lamellar structure ($0.54 > f_2 > 0.4$). The middle arrow of the vertical line $f_1 = 1$ corresponds to $f_2 = 0.5$. Here we have a diblock copolymer bilayer separating homopolymer domains, shown in Figure 12. This lamellar structure is characterized by large A domains composed of A homopolymers, separated by a lamellar structure of the diblock copolymers. The B blocks of the diblock copolymers form a bilayer structure. This Helfrich-like structure[18] is stable over a large part of the phase diagram but has a shallow free-energy minimum in the region around $f_1 = 1$ and $f_2 = 0.5$. For comparison, the free energy as a function of the lattice spacing d is shown in Figure 13 for $f_1 = 1.0$ and $f_2 = 0.5$ and for the symmetric diblock case with $f_1 = 0.5$ and f_2

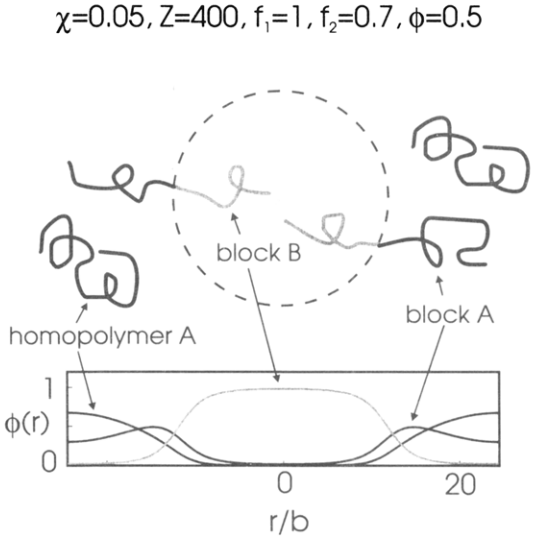

Figure 11. Structure−density profile diagram for a mixture of a homopolymer and an asymmetric diblock copolymer resulting in spherical domains, corresponding to the upper arrow on the vertical line $f_1 = 1$ shown in Figure 7.

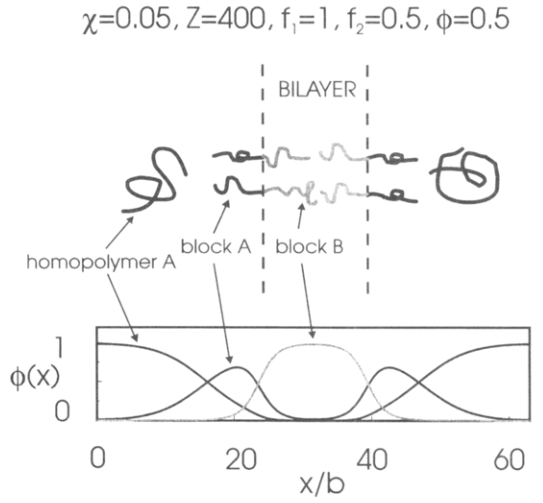

Figure 12. Structure−density profile diagram for a mixture of a homopolymer and a symmetric diblock copolymer resulting in diblock bilayers, corresponding to the middle arrow on the vertical line $f_1 = 1$ shown in Figure 7.

$= 0.5$. It is expected that fluctuations about the ordered state will be more significant for the shallow free energy with $f_1 = 1$ and $f_2 = 0.5$ than for the symmetric diblock structure. For even smaller values of f_2 ($0.4 > f_2 > 0.23$), an inverse spherical structure is stabilized in the binary mixtures. The lowest arrow along the vertical line $f_1 = 1$ shown in Figure 7 corresponds to $f_2 = 0.4$. Here we find an inverse spherical phase, for which the density profiles are displayed in Figure 14. In this case, we have well-defined spherical domains, stabilized by the A blocks of the copolymers, with the B blocks forming the supporting matrix and the homopolymer A acting as a filler inside the spherical domains. Comparing Figure 7 for $\chi = 0.05$ with the corresponding phase diagram for the strongly segregated case shown in Figure 6 ($\chi = 0.2$), we see that the inverse spherical phase persists in roughly the same region around the edge of the phase diagram, except for a narrowing of the region of stability in the strongly segregated case. This phase may have some practical applications in forming structures in local, but not global, thermodynamic equilibrium, as discussed in the next section.

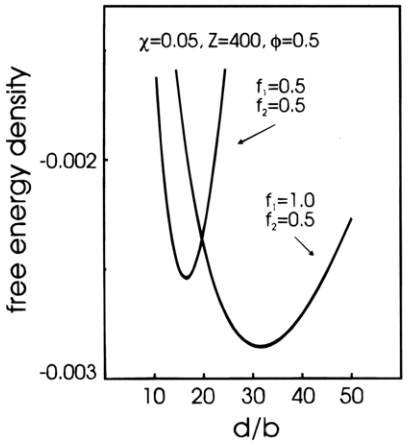

Figure 13. Free energy as a function of lattice spacing for a one-component system of symmetric diblocks with lamellar structure ($f_1 = 0.5, f_2 = 0.5$) and the bilayer lamellar structure ($f_1 = 1.0, f_2 = 0.5$), showing the shallower free energy minimum for the bilayer structure.

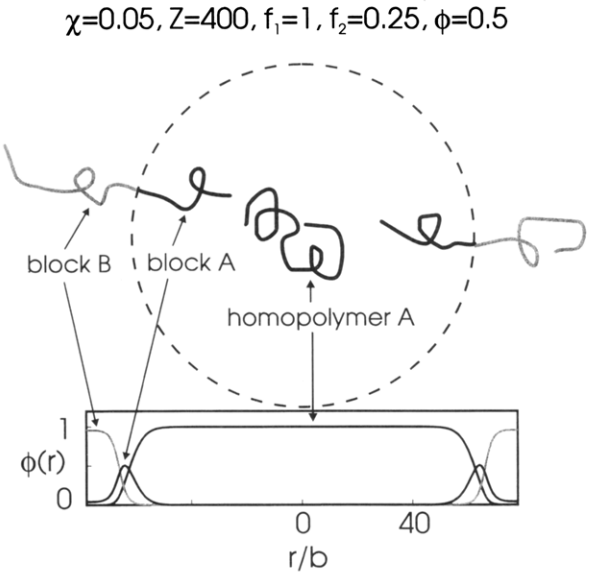

Figure 14. Structure−density profile diagram for a mixture of a homopolymer and an asymmetric diblock copolymer resulting in inverse spherical domains containing the homopolymer, corresponding to the lower arrow on the vertical line $f_1 = 1$ shown in Figure 7.

4. Inverse Spherical Structures in Local Equilibrium

An active area of research on materials suitable for electronic devices is the development of 3D optical memory devices.[17] The potential of an enormous information storage capability within a small volume and the possibility of moving the information in and out of storage rapidly make this an attractive research goal. There are numerous approaches to this problem; however, we will focus exclusively on the use of photochromic materials for 3D optical memory devices. The photochromic behavior of spiropyran derivatives dissolved in a polymer matrix or incorporated into the backbone of the bulk polymer has been discussed by Eisenbach[19] and by Smets.[20] In particular, many studies of the ring opening/closure of spirobenzopyrans involving cleavage of the C−O−pyran bond followed by rotation of one part of the molecule have been carried out. However, the purpose of this section is not to discuss the chemistry of this process but to point out that the inverse spherical structure shown in Figure 14,

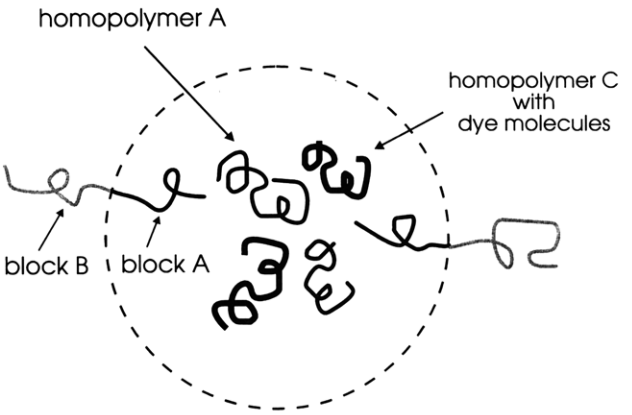

Figure 15. Schematic of inverse spherical structure similar to Figure 14, except that a homopolymer C (with attached dye molecules for possible 3D optical memory device applications) which is more incompatible with block B than with block A and homopolymer A is inside the domain, resulting in a structure which is in local, but not global, thermodynamic equilibrium.

which is stabilized by the presence of the homopolymer filler inside the spherical domains, may have a useful application as a possible structure for 3D optical memory device materials.

Figure 15 shows another version of the inverse spherical structure, in which the homopolymer A is complemented by another homopolymer C with attached dye molecules. For polymeric structures in local thermodynamic equilibrium it is not a requirement that homopolymer C be compatible with homopolymer A or block A of the copolymer; it is only necessary that homopolymer C to be more incompatible with block B of the copolymer than with homopolymer A or block A of the copolymer for the structure to remain in local equilibrium. Of course the preparation of such structures depends very much on the processing conditions, as has been observed before the three-component encapsulated homopolymer structures in local equilibrium.[21]

Other possibilities for dye attachment are to the A block of the copolymer or to homopolymer A. The best choice depends on the particular use of the material, the processing conditions, and the chemistry of the dye attachment. In any case, the controlled concentration of dye molecules into small spherical domains should offer a design advantage for the building of robust optical memory devices. Similar structures have been investigated by Cohen and co-workers for the purpose of incorporating metallic inclusions in a regular microscopic spatial array.[14−16]

5. Conclusions

The phase behavior of binary diblock copolymer mixtures is studied by using the self-consistent mean-field theory. Results for mixtures of long and short diblocks have been obtained earlier,[13] and mixtures of equal length diblocks are studied in this paper. A new scheme for phase structure analysis, the phase cube, has been presented for binary mixtures of diblock copolymers. The availability of the phase diagrams should provide useful guidance to the practical design of diblock copolymer blends for material applications. Although only a limited number of phases has been considered (lamellar, cylindrical, spherical), the results show where the phase boundaries are, and this should be useful in suggesting which regions could contain

more complicated structures. Conversely, the results also show that vast regions where the lamellar structure predominates, and these areas could be prudently avoided in searching for new structures. In addition, calculated density profiles are given for some interesting structures (inverse spherical, bilayer), and these could be investigated experimentally using techniques such as neutron reflectivity[22] or grazing incidence X-ray scattering.[23] Also, inaccuracies inherent in the inhomogeneous Flory–Huggins model are expected, especially for cases of substantial chain stretching, and the theoretical results here can be used to select structures which should also be investigated by other theoretical methods.[24] Finally, there is some practical value in knowing in what range of chain parameters the inverse spherical structure might be stable, especially if these structures are suitable for preparing metallic, semiconducting, or dye nanoclusters.[14-16]

Acknowledgment. J.N. thanks Professor Henri Benoit for a helpful discussion.

References and Notes

(1) Hajduk, D. A.; Harper, P. A.; Gruner, S. M.; Honeker, C. C.; Kim, G.; Thomas, E. L.; Fetters, L. J. *Macromolecules* **1994**, *27*, 4063.
(2) Vilesov, A. D.; Floudas, G.; Pakula, T.; Melenevskaya, E. Y.; Birshtein, T. A.; Lyatskaya, Y. V. *Macromol. Chem. Phys.* **1994**, *195*, 2317.
(3) Baek, D. M.; Han, C. D.; Kim, J. K. *Polymer* **1992**, *33*, 4821.
(4) Saito, R.; Kotsubo, H.; Ishizu, K. *Polymer* **1994**, *35*, 1580.
(5) Koizumi, S.; Hasegawa, H.; Hashimoto, T. *Macromolecules* **1994**, *27*, 4371.
(6) Hashimoto, T.; Koizumi, S.; Hasegawa, H.; Izumitani, T.; Hyde, S. T. *Macromolecules* **1992**, *25*, 1433.
(7) Löwenhaupt, B.; Steurer, A.; Hellmann, G. P.; Gallot, Y. *Macromolecules* **1994**, *27*, 908.
(8) Leibler, L. *Macromolecules* **1980**, *13*, 1602.
(9) Semenov, A. N. *Sov. Phys. JETP* **1985**, *61*, 733.
(10) Vavasour, J. D.; Whitmore, M. D. *Macromolecules* **1992**, *25*, 2041. Shull, K. R. *Macromolecules* **1992**, *25*, 2122. Matsen, M. W.; Schick, M. *Phys. Rev. Lett.* **1994**, *72*, 2660.
(11) Birshtein, T. M.; Liatskaya, Yu. V.; Zhulina, E. B. *Polymer* **1990**, *31*, 2185. Zhulina, E. B.; Birshtein, T. M. *Polymer* **1991**, *32*, 1299. Zhulina, E. B.; Lyatskaya, Yu. V.; Birshtein, T. M. *Polymer* **1992**, *33*, 332. Lyatskaya, Yu. V.; Zhulina, E. B.; Birshtein, T. M. *Polymer* **1992**, *33*, 343. Birshtein, T. M.; Lyatskaya, Yu. V.; Zhulina, E. B. *Polymer* **1992**, *33*, 2750.
(12) Dan, N.; Safran, S. A. *Macromolecules* **1994**, *27*, 5766.
(13) Shi, A.-C.; Noolandi, J. *Macromolecules* **1994**, *27*, 2936.
(14) Sankaran, V.; Cohen, R. E.; Cummins, C. C.; Schrock, R. R. *Macromolecules* **1991**, *24*, 6664.
(15) Sankaran, V.; Yue, J.; Cohen, R. E.; Schrock, R. R.; Silbey, R. *J. Chem. Mater.* **1993**, *5*, 1133.
(16) Yue, J.; Sankaran, V.; Cohen, R. E.; Schrock, R. R. *J. Am. Chem. Soc.* **1993**, *115*, 4409.
(17) Dvornikov, A. S.; Malkin, J.; Rentzepis, P. M. *J. Phys. Chem.* **1994**, *98*, 6746.
(18) Helfrich, W. *J. Phys. (Fr.)* **1985**, *46*, 1263.
(19) Eisenbach, C. D. *Ber Bunsen-Ges. Phys. Chem.* **1980**, *84*, 680.
(20) Smets, G. *Adv. Polym. Sci.* **1983**, *50*, 18.
(21) Hobbs, S. Y.; Dekkers, M. E. J.; Watkins, V. H. *Polymer* **1988**, *29*, 1598.
(22) Russell, T. P.; Menelle, A.; Hamilton, W. A.; Smith, G. S.; Satija, S. K.; Majkrzak, C. F. *Macromolecules* **1991**, *24*, 5721.
(23) Factor, B. J.; Russell, T. P.; Toney, M. F. *Macromolecules* **1993**, *26*, 2847.
(24) Binder, K.; Fried, H. *Macromolecules* **1993**, *26*, 6878.

MA946087O